Effect of turbulence on feeding of larval fishes: a sensitivity analysis using an individual-based model

Bernard A. Megrey and Sarah Hinckley

Recent research has shown that turbulence can be important in the feeding of larval fishes. The interplay of turbulence with other important factors affecting larval feeding and growth rates is less known because of the difficult problems associated with multi-factor *in situ* experiments. We use an individual-based model (IBM) of the early life stages of walleye pollock (*Theragra chalcogramma*) to examine the sensitivity of growth and mortality to turbulence. This probabilistic and mechanistic model follows individual fish through the egg, yolk-sac larvae, feeding larvae, and juvenile stages, and includes development, behaviour, feeding, bioenergetics, and growth for each life stage. Biological processes are driven by physical factors (temperature, salinity, and turbulence) derived from a companion hydrodynamic model and configured for environmental conditions prevalent in 1987. A foraging submodel explicitly incorporates the effect of turbulence, prey density, and larval size. Monte Carlo simulations using Latin Hypercube Sampling methods were used to perform a sensitivity analysis. The error analysis examines the relative importance of various feeding-related factors on larval growth and mortality. Model results conform to wind-induced turbulence/contact-encounter rate theory with maximum consumption rates occurring at wind-speeds of $7.2 \, \text{m s}^{-1}$. Reactive distance, minimum pursuit time, and weight-length conversion parameters were the most important input parameters affecting the turbulence-consumption processes. The rank order of important input parameters shows that the weight–length conversion power coefficient and reactive distance (directly through the reactive distance–length proportionality coefficient) were two factors that influenced the largest number (17 out of 24) and largest percentage (71%) of output variables. Feeding depth was ranked third, influencing 50% of the output variables. Our results show that smaller and younger larvae are more sensitive to turbulent effects than are larger and older larvae.

Keywords: fish larvae, Latin Hypercube Sampling, wind-induced turbulence.

Bernard A. Megrey and Sarah Hinckley: National Oceanic and Atmospheric Administration, National Marine Fisheries Service, Alaska Fisheries Science Center, 7600 Sand Point Way NE, Seattle, WA 98115, USA; Tel: +1 206 526 4147; Fax: +1 206 526 6723; e-mail: bern.megrey@noaa.gov

Introduction

It is well established that wind-induced small-scale turbulence in the sea affects marine plankton ecology on many levels. Sundby *et al.* (1995) point out that any wind event can change many oceanic variables affecting larval fish, such as advection/retention, vertical mixing, entrainment, upwelling, frontal structures, plankton contact rates, buoyancy, temperature, and light conditions. The influence of turbulence on larval fish, as planktonic organisms, has been the topic of research since the mid-1970s. Early theory on the effect of winds and storms on larval fish growth, survival, and

recruitment focused on dispersion of prey patches, dilution of prey (Lasker, 1975; Peterman and Bradford, 1987) and effects on prey production, for example, through enhancement of upwelling or wind-induced mixing (Cury and Roy, 1989; Cury *et al.*, 1995). More recently, theory has focused on turbulence as an important factor affecting the feeding process, through its effect on increasing larva–prey encounter rates (Rothschild and Osborn, 1988; Marrase *et al.*, 1990; Matsushita, 1991) and decreasing the probability of successful pursuit (MacKenzie *et al.*, 1994). Recently, Dower *et al.* (1997) provided a complete chronological development of the theory of the effects of microscale turbulence on

the feeding ecology of marine fish larvae. This body of work provides a theoretical framework for assessing the mechanisms of how winds and storminess may affect the feeding, growth, and survival of individual larvae, and possible relationships to recruitment.

Our objective is to use simulation as a framework to examine which parameters are most important in determining the effect of turbulence on feeding of fish larvae and to determine the relative effect of turbulence on overall rates of growth and survival.

We chose to use simulation modelling to examine this problem because it is extremely difficult to generate and measure realistic turbulent energy spectra in the laboratory, measure turbulence in the field (Gargett, 1989), and to measure prey and larval parameters on appropriate time and space scales in the laboratory or the field. More importantly, the effects of turbulence on planktonic organisms are not well understood, mainly because many aspects of the theoretical framework are still insufficiently explored (Werner et al., 1995; Dower et al., 1997; Sundby, 1997). The necessity for a modelling approach to describe and analyse the turbulence/plankton encounter rate/consumption process is especially clear when considering the potential and actual interactions of important biological and physical components of the process and the fact that the problem is well beyond description in a closed analytical mathematical formulation.

We chose individual-based models (IBM; Huston et al., 1988; DeAngelis and Gross, 1992; Judson, 1994) as opposed to aggregate models because biophysical processes related to turbulence and the fundamental way it affects larval feeding occur at the scale of individual fish and their prey. Thus, characteristics of individual fish (length, depth, and the prey field they see) are critical to describing and analysing processes relevant to turbulence. IBMs are sufficiently flexible to accommodate a wide range of time and space scales and can easily describe biological processes for individuals or aggregated populations. They can also easily incorporate individual larval and prey behaviour as well as the required mathematical and computational complexity. The use of sensitivity analysis in large process-oriented early life history simulation models is not new (Werner et al., 1995; Letcher et al., 1996). We used a Monte Carlo sensitivity analysis to address specifically the problem of larval feeding in calm and turbulent environments and the effect of turbulence on growth and survival.

The approach has been applied to pollock in Shelikof Strait, one of the major spawning areas in the Gulf of Alaska (Hinckley et al., 2001; this volume) by combining the IBM model with a hydrographical circulation model and a nutrient–phytoplankton–zooplankton model (Hinckley et al., 1996; Hinckley, 1999).

Materials and methods

General

The IBM used (Hinckley et al., 1996) follows individuals from spawning through egg, yolk sac, and feeding larval stages. Each stage has stage-specific descriptions of development, growth, mortality, feeding, and bioenergetic processes. The model also includes individual behaviour such as vertical migration. The section of the model describing the feeding larval life stage was modified to accommodate detailed descriptions of the turbulence/contact rate process. Generally, processes of this stage include descriptions of total mortality as a function of length, starvation mortality as a function of condition, consumption as a function of prey parameters and wind-generated turbulence, and growth as a function of consumption, metabolism, and temperature. The consumption process was enhanced considerably over the description given in Hinckley et al. (1996).

Where possible, descriptions of the wind-induced turbulence/prey encounter model are provided by reference to the original publication(s) by equation number. Descriptions of variable and parameter names, and corresponding units, are given in Appendix 1.

Consumption

The consumption process is formulated as a deterministic function of four main factors: prey density, wind-generated turbulence, encounter rate, and probability of successful pursuit. Most factors are functions of larval body size. Rothschild and Osborn (1988) proposed the idea that the relative velocity between planktonic larval fish and their prey may be enhanced by turbulence in the ocean, thus increasing contact rates. This idea has been explored further by MacKenzie and Leggett (1993) and Sundby and Fossum (1990). MacKenzie et al. (1994) added post-encounter components of consumption (pursuit, attack, and capture) to the contact rate model. The response of these two conceptual models to increasing turbulence balances the positive effects of increased contact rate and the negative effects of increased pursuit time. The result is a dome-shaped consumption versus turbulence curve where there is a windspeed that results in an optimal level of turbulence. As turbulence increases beyond the optimal level, contact rate increases but pursuit time becomes a limiting factor and larval feeding rate decreases.

We used the MacKenzie et al. (1994) formulation modified by taking into account our assumption that larval pollock appear to be pause-travel predators rather than cruise predators (MacKenzie and Kiørboe, 1995). The encounter probability was therefore modified to reflect the laboratory observation that larvae only search for food when they are motionless (S. Spring,

pers. comm.). Consumption, in micrograms dry weight consumed per day per individual fish, is the product of the number of prey encountered per day and the probability of successful pursuit. The formulation describing the number of prey encountered per day is taken from Equation (1b) [hereafter referred to as (1)] in MacKenzie and Kiørboe (1995), where E_s=encounter rate (prey s^{-1}), R=reactive distance (m), N=prey density (no. m^{-3}), μ=prey velocity (m s^{-1}), Ω=turbulent velocity (m s^{-1}), PF=pause frequency (no. s^{-1}), and PD= pause duration (s). This formulation assumes that the larva scans the half sphere directly in front of it, with a radius equal to its detection range. Also included is the added rate of encounter with prey that are advected or that swim into this half sphere.

Turbulent velocity is a function of the dissipation rate and a length scale (Rothschild and Osborn, 1988). We use Equation (4) of MacKenzie and Kiørboe (1995) for this formulation [hereafter referred to as (2)], where R is assumed to be the proper length scale and ε is the dissipation rate of turbulent kinetic energy (m s^{-3}). The dissipation rate at any depth (ε, W m^{-3}), which is described by Equation (10) [hereafter referred to as (3)] of MacKenzie et al. (1994), is calculated from windspeed, where z=depth (m) and W=windspeed (m s^{-1}). This assumes that the larvae are in a well-mixed layer, and therefore turbulence levels below the model mixed layer may be overestimated. Similar to Tilseth (1984), we represent larval reactive distance (r, mm) as a function of larval length (l, mm):

$$r=RDA\ l \qquad (4)$$

where RDA is the slope of the reactive distance–length relationship. Note that r is expressed in millimetres, while R in (1) and (2) is in metres.

Each volume of water scanned during a pause is assumed to be independent of the last volume of water scanned. Then,

$$E_d=EY=(3600\ s\ h^{-1})\ HRLIGHT \qquad (5)$$

where E_d=encounter rate (prey d^{-1}) and HRLIGHT=hours of daylight. Feeding is assumed to occur only during daylight hours, based on laboratory (Paul, 1983) and field observations (Canino and Bailey, 1995).

Development of the model for the probability of successful pursuit is detailed in MacKenzie et al. (1994). In short, the model assumes that the probability of successful pursuit (the prey approach and fixation time) is the most sensitive of the post-encounter processes to the negative effects of turbulence. A coordinate system centred on the larval eye is defined, with the larva considered fixed in space (with only relative motion between larva and prey considered important). Turbu-

lence is assumed to be locally isotropic within the larval encounter distance. The distance that the prey can be moved by turbulent motion, once it has been spotted by the larva, is turbulent velocity (ω, mm s^{-1}) times minimum pursuit time (t, s), which defines the prey encounter sphere. The model defines the likelihood that the prey will remain within the larval encounter sphere once it has been spotted (given that it is in a turbulent regime) for at least the minimum pursuit time. The probability of successful pursuit Pr(sp) is described by Equation (2) [hereafter referred to as (6)] in MacKenzie et al. (1994) as the ratio of the volume of overlap between the prey excursion sphere and the larval encounter sphere V_{over} to the total volume of the prey excursion sphere V_{prey}.

Equation (6) is solved for all values of a, the encounter distance between a larva and a prey item [Equation (6) in MacKenzie et al. (1994); hereafter referred to as (7)]. The solution to (7) has three valid domains (ωt<r; r<ωt<2r; ωt>2r). The expression of this formulation for the three domains is presented in MacKenzie et al. (1994) as Equations (8a), (8b), and (8c). The solution to these equations is given by Equations (8), (9), and (10):

$$\begin{aligned}
Pr(sp)_{\omega t<r}=&\{(12r^3\cdot t\cdot\omega)+(6r^2\cdot t^2\cdot\omega^2)\\
&+(44r\cdot t^3\cdot\omega^3)-(21t^4.\omega^4)\\
&-(12r^4.logr)+(24r^2\cdot t^2\omega^2\cdot logr)\\
&-(12t^4\cdot\omega^4\cdot logr)+[12r^4\cdot\log(r-t\cdot\omega)]\\
&-[24r^2\cdot t^2\cdot\omega^2\cdot\log(r-t\cdot\omega)]\\
&+[12t^4\cdot\omega^4\cdot\log(r-t\cdot\omega)]\}/(64r\cdot t^3\cdot\omega^3) \quad (8)
\end{aligned}$$

$$\begin{aligned}
Pr(sp)_{r<\omega t<2r}=&\{(12r^3\cdot t\cdot\omega)+(6r^2\cdot t^2\cdot\omega^2)\\
&+(44r\cdot t^3\cdot\omega^3)-(12t^4\cdot\omega^4)\\
&-(12r^4.logr)+(24r^2\cdot t^2\cdot\omega^2\cdot logr)\\
&-12t^4\cdot\omega^4\cdot logr\\
&+[12r^4\cdot\log(-r-t\cdot\omega)]\\
&-[24r^2\cdot t^2\cdot\omega^2\cdot\log(-r+t\cdot\omega)]\\
&+[12t^4\cdot\omega^4\log(-r+t\cdot\omega)]\}/\\
&(64r\cdot t^3\cdot\omega^3) \quad (9)
\end{aligned}$$

$$Pr(sp)_{\omega t>2r}=r^3/(\omega\cdot t)^3 \qquad (10)$$

Prey swimming speeds are calculated using the estimate (Sundby and Fossum, 1990) of 0.5 body lengths per second measured on adult *Euphausia pacifica* by Torres and Childress (1983). Using estimates of median body width for naupliar (0.20 mm) and copepodite (0.90 mm) groups, swimming speeds for these stages were estimated to be 0.00010 and 0.00045 m s^{-1}, respectively. Eggs were assumed to be motionless.

Pause frequency and duration parameters were derived from laboratory experiments on larval cod feeding and swimming patterns at different food densities (adapted from MacKenzie and Kiørboe, 1995). Pause frequency (PF) is a constant. Pause duration (PD) is

made a linear function of larval length (l) and contingent on the ambient turbulence condition and prey density (PREY; for definition of other symbols see Appendix 1) based on the following decision rule:

if ε<CALM then
  if PREY<LOWPREY then PD=PD1A+PD1B·l
    elseif l⩾PD2A/PD2B then PD=PD2A+PD2B·l
    else PD=BIGPD
elseif PREY<LOWPREY then
  if l PD3A/PD3B then PD=PD3A+PD3B·l
    else PD=BIGPD
  if l PD4A/PD4B then PD=PD4A+PD4B·l
    else PD=BIGPD

Values of windspeed are input for each larval location using a general circulation model for the Shelikof Strait region (SPEM; Semispectral Primitive Equation Model) for each year (Stabeno et al., 1995). This data set consists of average daily geotriptic winds computed from six-hourly atmospheric surface pressure measurements contributed by the Fleet Numerical Oceanographic Center (FNOC). These geostrophic winds were rotated 15° counterclockwise, the speeds were reduced by 30%, and the results interpolated to the hydrodynamic grid (Macklin et al., 1993). For a specified range of wind directions, the geotriptic winds must be modified to account for ageostrophic winds, which can be common in Shelikof Strait (Lackman and Overland, 1989; Macklin et al., 1993). An algorithm that has been developed from observations is applied to the geotriptic winds to account for the channelling and enhancement of winds within the Strait.

Prey densities are read into the IBM model using the output (average daily numbers m^{-3} of each *Pseudocalanus* stage at the larval depth) from a deterministic Nutrient–Phytoplankton–Zooplankton (NPZ) model similar to that described in Frost (1987, 1993). The wind and prey field data sets use the same 20 × 20 fixed Eulerian spatial grid used by the NPZ model, which is a subset of the SPEM grid (Hinckley, 1999; Hinckley et al., 2001, this volume). The windspeed and prey density at each larval location is linearly interpolated using values from nearby grid points.

The maximum size of prey items (maxprey) taken by a larva of length (l) is given by (Nishiyama et al., 1993):

$$\text{maxprey}=0.0115 \cdot e^{(0.235 \cdot l)} \tag{11}$$

This maximum size is converted into the maximum stage of *Pseudocalanus* (maxstage) taken using a maximum carapace length for each stage (J. Napp, pers. comm.). Prey of the size taken by the larva are aggregated into three groups: eggs, nauplii, and copepodites. The probability of a larva of length l taking prey consisting of
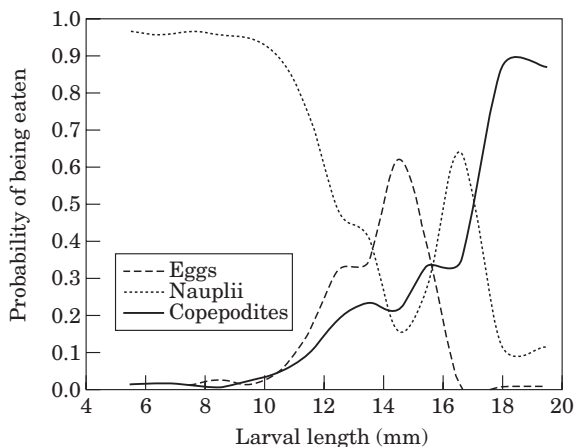

Figure 1. Relationship between the probability of being eaten for three prey categories (eggs, nauplii, and copepodites; adapted from Kendall et al., 1987) and larval pollock length.

eggs, nauplii, or copepodites is determined using data from Kendall et al. (1987).

The encounter rates of a larva with eggs, nauplii, and copepodites are calculated separately. Then the probability of successful pursuit is determined using (8), (9), or (10). The appropriate equation used will be dependent on larval length and location. The number of items consumed (C_i for i=eggs, nauplii, or copepodites) is calculated as:

$$C_i=E_i \cdot Pr(sp) \cdot Pr(eat)_i \tag{12}$$

Where E_i is the number of prey items encountered, Pr(sp) is the probability of successful pursuit, $Pr(eat)_i$ is the probability of larva eating i. The probability of a larva eating an egg, nauplii, or copepodite varies as a function of larval length [Figure 1; from Kendall et al. (1987)].

The dry weight of prey items is calculated using the values for each stage, assuming that numbers consumed are distributed equally among all stages in that group. The total consumption (dry weight d^{-1}) for the larva is the number consumed of each prey stage, converted to dry weight of each group consumed, and summed over prey stages.

Total consumption (C, μg) is used in the calculation describing daily weight change as follows

$$W_{j+1}=W_j+AELARV \cdot C+TR \tag{13}$$

where W is larval dry weight (μg), AELARV is assimilation efficiency, TR is total daily respiration rate (μg dry wt d^{-1}), and j denotes day of year. Weight is converted to length using Equations (13) and (14) in Hinckley et al. (1996).

Mortality

One problem of using stochastic IBMs to study processes affecting early life stages is trying to account computationally for enough individuals to result in a statistically significant number of individuals remaining at the end of the simulation, especially in a spatial context. Extremely high mortality rates in the different larval stages mean that the total number of individuals is quickly reduced as they progress through their life stages, while computational limitations (e.g. memory) constrain the number of individuals that can be reasonably modelled.

Several ways of dealing with this problem have been devised. Rose *et al.* (1993) described a re-sampling algorithm that replaces individuals lost with a randomly chosen surviving member of the population (donor individual). This method follows a fixed number of individuals, each representing some number of identical population members. The number of individuals represented by one donor individual is adjusted to represent the loss of individuals caused by mortality. The dead individual's attributes are replaced by those of the donor individual. This method will not work with spatially explicit modelling, because individuals from different locations vary because of differences in the environment experienced over time: random choice of one of the surviving individuals would bias the spatial information contained in the model.

A second way of dealing with this problem has been called the "superindividual" method (Scheffer *et al.*, 1995) and a modified version has been implemented in our model. An "individual" represented by a point in space actually becomes a "superindividual" or cohort, the members of which experience the same velocity, temperature, salinity, and prey conditions. Feeding, metabolism, and growth of each cohort are assumed to be the same. This assumption is appropriate, given the goals of the exercise. We are mainly interested in differences at the mesoscale spatial level, and this method preserves these differences by assuming that individuals located at the same place experience the same conditions.

A variable called "value" (V) is defined for each individual that is set at the beginning of the simulation to a number representing the initial number in the cohort. This initial value is reduced each day by mortality. The instantaneous daily mortality rate experienced by an individual on each day is a random deviate from a triangular distribution whose minimum, mean, and maximum differ by life stage and/or larval length. The mean mortality rate for feeding larvae 7.0 mm is a function of length. This relationship was derived from age-mortality information (Bailey *et al.*, 1996) and length-at-age information (S. Picquelle, pers. comm.) derived from walleye pollock larvae sampled at the same

locations and times. The variable V is updated each day (j) using the equation:

$$V_{j+1} = V_j \cdot e^{-nmort} \qquad (14)$$

where nmort (d^{-1}) represents an estimate of the total daily mortality rate. Starvation mortality is calculated based on comparison to a critical condition factor (CRITKFDL), which was set equal to the minimum condition factor seen in larval length–weight data (K. Bailey and D. Siefert, pers. comm.).

Estimates of total mortality rate are based on larval length (l) using a mortality–age relationship (Bailey *et al.*, 1996), length–age parameters for 1987, and the following decision rule:

nmort = $e^{-(MSIZEA1-MSIZEB1 - ln l)}$
if length <7mm then nmort=MFDLSM
elseif age >25 days then nmort=OLDMORT
elseif nmort <0.02 d^{-1} then nmort=MINMORT

An estimate of predation mortality was calculated as the difference between total mortality and starvation mortality.

Sensitivity analysis

The sensitivity analysis involved a Monte Carlo simulation wherein model input parameters are drawn from a random distribution in each run. The analysis was implemented using a Latin Hypercube Sampling (LHS; McKay *et al.*, 1979) procedure in a three-step procedure. The first step involved generating a suite of random input parameter values; the second was running the simulation model to generate a set of output variables. The simulation was executed numerous times to generate a set of replicated model input parameter and output variable observations. Finally, the third step involved the statistical analysis of the model input parameters and output variables. Partitioning the variance of an output variable into contributions from all input parameters suggests which input parameter has the largest influence on the output variable.

LHS was selected because it provides a powerful though relatively obscure method to perform a sensitivity analysis. A LHS error analysis is based on a type of stratified sampling scheme and differs from the usual individual parameter perturbation because all model input parameters are modified simultaneously during each run instead of increasing or decreasing one parameter at a time by a fixed amount. A set of input parameters, typically considered fixed in value, is represented as random variates drawn from an assumed probability distribution. Similarly to Letcher *et al.* (1996), we adjusted model variables, results of computations, as well as parameters of empirical relationships.
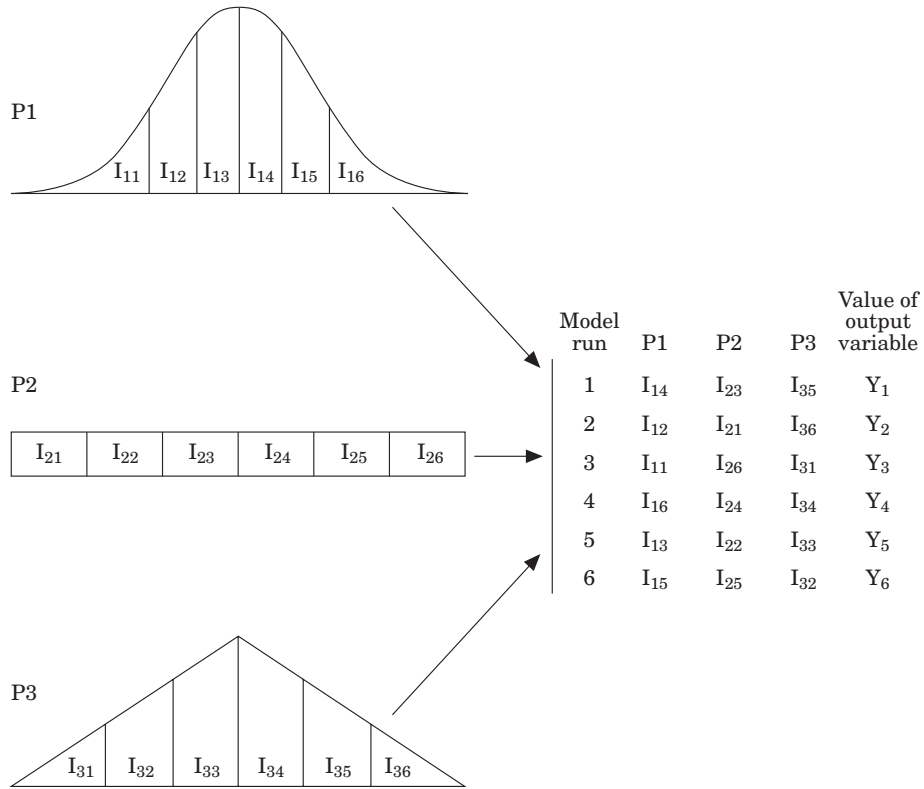
Figure 2. Theoretical schematic cartoon of a Latin Hypercube Sample sensitivity analysis (adapted after Rose, 1981) for three parameters characterized by a normal (P1), rectangular (P2), and triangular (P3) distribution (see the text).

If simple random sampling were used, parameter values could cluster and regions in the random parameter space might develop from which no parameter values were sampled. The result would be redundancy in the information of the model runs. A stratified sampling method was used to avoid this problem, because it ensures more even coverage by dividing the parameter space into sections and sampling from each section with a certain probability. In LHS, the number of runs is determined by the number of intervals forming the probability distributions, regardless of the number of parameters in the model. In each run, every input parameter distribution is sampled. A useful property is that the number of runs required is independent of the number of parameters.

Sensitivity is evaluated with rank correlation or simple correlation depending on whether covariance exists between the input parameters. The premise underlying the use of this statistic is that the greater the correlation between the parameter and the output variable (% variance explained in the output variable by the parameter), the more influence the parameter has in controlling model behaviour (Rose *et al.*, 1991). Figure 2 shows a theoretical schematic cartoon of a LHS sensitivity analysis made up of six replicate Monte Carlo runs of the simulation model using a random suite of three input parameters and the response of one output variable. Input parameters are described by the normal, uniform, and triangular probability distributions. Each input parameter distribution P_j is divided into six intervals I_{jk}, $k=1,\ldots,6$. All intervals contain an equal area under the assumed probability density function. Intervals are randomly assigned to simulations so that each interval appears in only one run. Within an input parameter distribution, a single value is randomly sampled from each interval, assuming a uniform distribution over the interval. This assumption of uniformity is valid because the intervals were constructed so that all contain an equal area under the distribution. We used simple correlation statistics (Pearson's R) to analyse the results. The premise underlying the use of a Pearson's R is that the greater the correlation between the output variable and the input parameter, the more influence the parameter has in controlling model behaviour. Sensitivity is measured in terms of magnitude (absolute values) and the direction of the influence (sign). Because no covariance relationship among the input parameters was specified in the application described here, the parametric r^2 can be used to evaluate sensitivity.
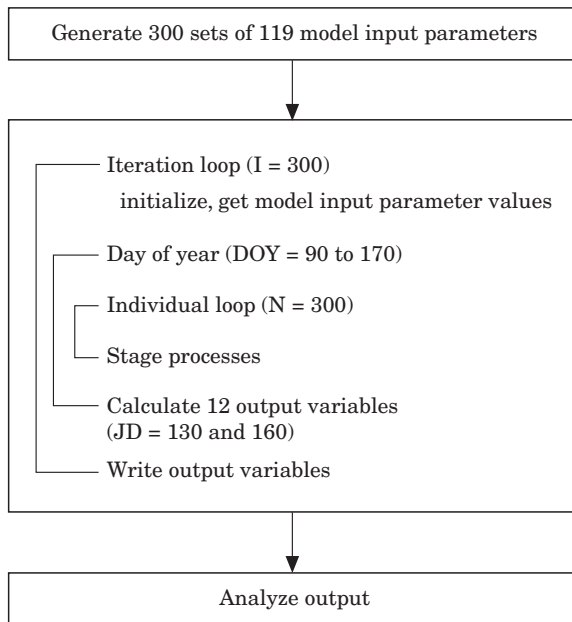
Figure 3. Flow diagram of the sensitivity analysis and simulation process. Most stage processes depend on larval size.

Table 1. Description of IBM output variables (for DOY 130 and 160).

Output variable	Description
MCFLL	Mean cumulative feeding (μg dry wt d^{-1}), large larvae
MCFSL	Mean cumulative feeding (μg dry wt d^{-1}), small larvae
MGR	Mean instantaneous growth rate (d^{-1})
MLEN	Mean length (mm)
MMD	Mean metamorphosis date
MNO	Mean number of surviving individuals (number)
MPSLL	Mean probability of successful pursuit, large larvae
MPSSL	Mean probability of successful pursuit, small larvae
MPZ	Mean instantaneous predation mortality rate (d^{-1})
MSZ	Mean instantaneous starvation mortality rate (d^{-1})
MWT	Mean weight (g)
MZ	Mean instantaneous total mortality rate (d^{-1})

Simulations

The sensitivity analysis examined the importance of 119 parameters describing the feeding dynamics (the consumption-turbulence process), growth, mortality and depth distribution of the larval stage only; 15 parameters dealt with bioenergetic calculations such as energy transfer efficiencies and weight–length conversions; 18 parameters described the mortality process including larval mortality–size functions, base mortality, and starvation and predation mortality; and the consumption–turbulence formulation needed 86 parameters to describe the probability of eating eggs, nauplii, and copepodites (14 size groups), larval pause duration (four combinations of size groups and ambient turbulence condition and prey density), prey weight, diel larval migration, turbulent diffusion and velocity, prey speed, and encounter probability.

The complete simulation process is described schematically in Figure 3. Three hundred data sets were generated. Within each set, random variates for each of the 119 input parameters were drawn from a triangular distribution. This distribution was used because it approximates a normal distribution yet does not require an estimate of variance. This consideration was important because variance estimates for most of the input parameters were not available, and it was easier to provide a mean, minimum, and maximum value (minimum information requirements for describing triangular probability density functions; note that this function is not required to be symmetric). Random variates for each

input parameter were independent among the 300 data sets. Input parameters and their nominal values are given in Appendix 1.

Output variables were arbitrarily selected so as to maximize the ability to ascertain any time dependence of the sensitivity conclusions, determine important aspects of model behaviour, provide information for judging parameter importance, and to evaluate overall model response to changes in the input parameters. Output variables were calculated for two days of the year: DOY 130 (10 May) and DOY 160 (10 June). On these two days, 24 output variables were computed (Table 1). In addition, two output variables (cumulative consumption and average probability of successful pursuit) were also calculated for small and large larvae (those having < average size and $\geq$ average size, respectively) on these dates.

The model was executed in three main loops. The innermost loop tracked 300 individuals and controlled all stage processes. The middle loop controlled the day of the year. The IBM was configured to execute a simulation running from DOY 90 (1 April) to DOY 170 (20 June). Within this loop, output variables were calculated on DOY 130 and 160. The outer loop iterated through the 300 input parameter sets. Within this loop, all model variables were initialized, input parameter values assigned, and input parameters and output variables were written to an output file. Finally, results contained in the output file were analysed.

Several external inputs were required in addition to the input parameter file. Input files of driving variables for 1987 included the prey field derived from the dynamic prey model resolved over time and depth. Larval prey (*Pseudocalanus* spp.) were resolved to all egg, naupliar, and copepodite stages. A wind field file, derived from FNOC modelled winds and corrected for
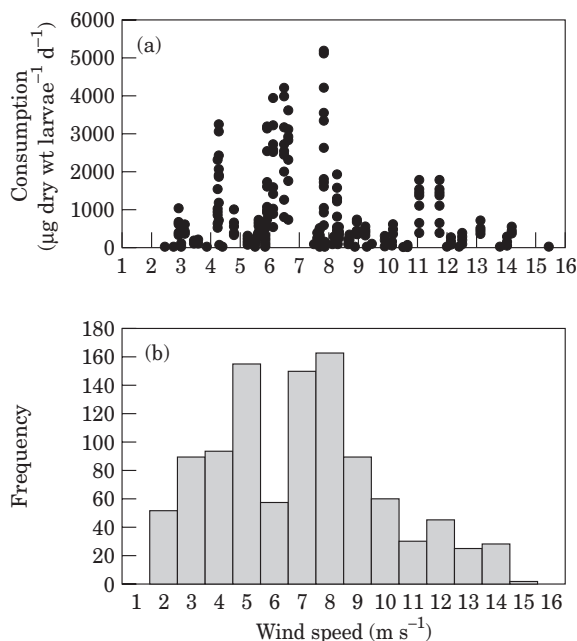
Figure 4. Model output showing a dome-shaped relationship between consumption and windspeed (a) and the frequency distribution of windspeed used to drive the model (b).

the region, was required to drive the turbulence equations. A temperature and salinity file, derived from SPEM (Hermann and Stabeno, 1996), resolved over depth and time, was required to drive temperature-dependent biological process and egg buoyancy calculations.

Results

We evaluate the performance of the IBM by examining the output with respect to the predicted influence of wind-generated turbulence on feeding. Output from the model (Figure 4) conforms nicely with the theory by the indication of a well-defined peak in consumption at intermediate windspeeds (MacKenzie et al., 1994). Because of the high variability in the model data, we estimated the wind speed that generated optimum consumption by fitting a quadratic line through windspeed and consumption data, averaged by Julian day over the period DOY 102–164, the period when larvae pollock are alive. The windspeed that generated maximum consumption (540 μg dry weight per day per individual) was estimated at 7.2 m s^{-1}.

Another measure of model performance was the relationship between starvation mortality and average probability of successful pursuit (Figure 5). These results indicate that starvation mortality decreases as probability of successful pursuit increases, with the decrease being more pronounced for older larvae (DOY 160). On
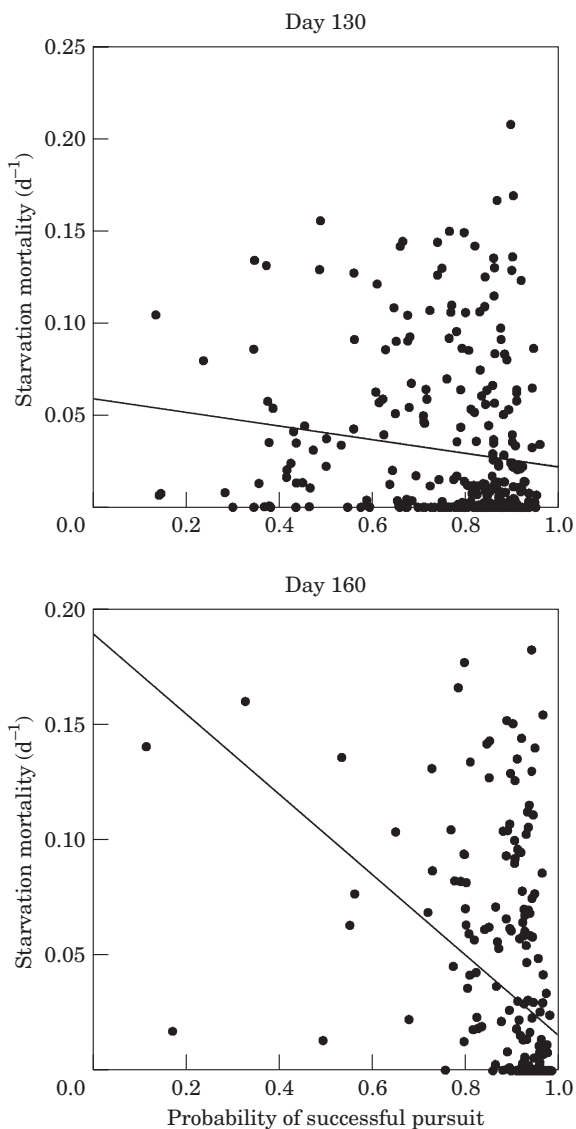
Figure 5. Model output indicating the relationship between starvation mortality and probability of successful pursuit for DOY 130 (top) and DOY 160 (bottom). Straight lines are linear fits to the data.

average, starvation mortality was lower for older larvae compared to young larvae. Older larvae were more successful, and less variable, at pursuing their prey, as indicated by the tendency of the data points to be clustered toward the right-hand side of the bottom panel.

The IBM generated copious amounts of information. Figure 6 shows one example of the magnitude and direction of the sensitivity of 24 output variables to one model input parameter: RDA, the slope of the reactive distance–length relationship. An output variable was considered sensitive to the input parameter (indicated by

Figure 6. Summary plot of the sensitivity of 24 output variables (cf. Appendix 1) to the input parameter RDA (reactive distance–length slope coefficient). Black and grey bars indicate that the output variable was sensitive ($r > 0.15$) and insensitive ($r < 0.15$), respectively, to the input variable.

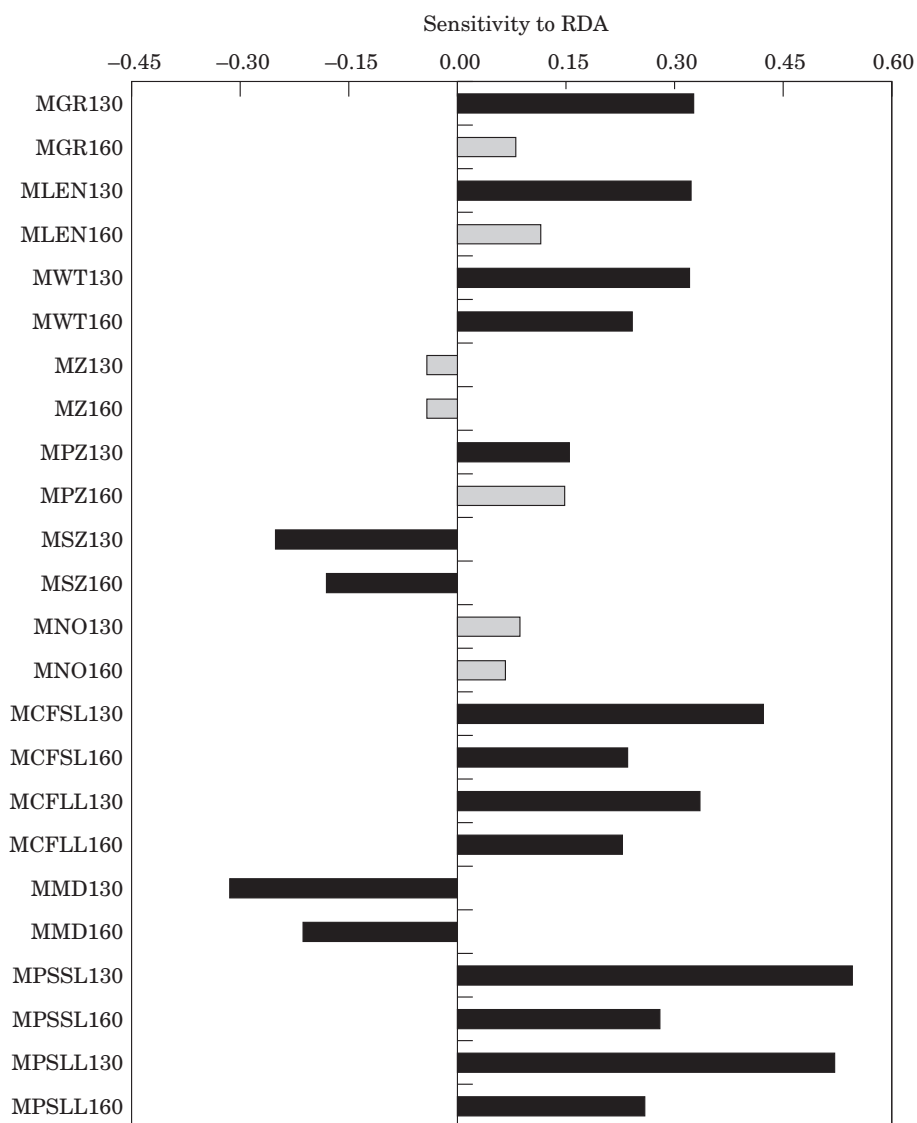a black bar) if the absolute value of the correlation coefficient was 0.15 (an approximation based on the critical value of 0.113 for a Pearson's R at $\alpha = 0.05$ and $n = 300$). These data show that increasing RDA significantly increased mean growth rate (MGR130), mean length (MLEN130), and mean weight (MWT130), but only for the young larvae (DOY 130) and increased mean cumulative feeding as well as mean pursuit time for small (MCFSL130, MCFSL160, MPSSL130, and MPSSL160) and large larvae (MCFLL130, MCFLL160, MPSLL130, and MPSLL160), on both DOY 130 and 160. Increasing RDA had a positive effect on mean numbers for both dates (MNO130 and MNO160), but

not to a significant degree. Increases in RDA caused significant decreases in mean metamorphosis date on both dates (MMD130 and MMD160). This is a consequence of increased growth; faster growing larvae will reach metamorphosis sooner. Increased reactive distance, through RDA, did not decrease mean total mortality to a significant degree (MZ130 and MZ160), although starvation mortality decreased significantly (MSZ130 and MSZ160). Also of note is a consistent trend that the effect of RDA on all output variables is more pronounced for young larvae compared to old larvae, regardless of the direction of the effect of the input parameter on the output variable.

Table 2. List of (a) input and (b) output parameters ranked by their influence on 24 output and 119 input parameters, respectively.

	Number	% of total
a. Sensitive output variables		
Input parameters		
LWYBB	17	71
RDA	17	71
FDEPTHG	12	50
MROFDLB	10	42
MAXPREYA	8	33
MFDLSM	8	33
WA	7	29
b. Sensitive input parameters		
Output variable		
MMD130	39	29
MMD160	28	20
MPZ130	11	8
MSZ160	10	7
MLEN130	9	7
MPZ160	9	7
MSZ130	8	6

Sensitivity was more generally evaluated by considering which input parameters significantly influenced output variables and which output variables were most influenced by the suite of input parameters (Table 2). The rank order of important input parameters controlling model behaviour [Table 2(a)] shows that the weight–length conversion power coefficient (LWYBB) and slope of the reactive distance–length relationship (RDA) were two that influenced the largest number of output variables (71%). Larval feeding depth (FDEPTHG) was ranked third, influencing 50% of the output variables. The routine metabolism power coefficient (MROFDLB) ranked fourth, followed by the intercept parameter of the larval length–maximum prey size function (MAXPREYA), the base mortality when larval length is less than 7 mm (MFDLSM), and the proportionality constant in the turbulent velocity function (WA). The rank order of important output variables [Table 2(b)] shows that mean metamorphosis date on both DOY 130 (MMD130) and 160 (MMD160) was sensitive to 39 and 28 input parameters out of a total of 119, respectively. Four out of the next five ranked output variables, dealing mainly with starvation and predation mortality, were sensitive to 6–8% of the input parameters.

A summary of sensitivity results, organized by process, day of the year, and output variable is presented in Table 3. Within the growth process, on DOY 130 the input parameters most influencing the growth, length, and weight processes were identical. Reactive distance–length relationship slope coefficient (RDA) had a similar positive effect on growth, length, and weight processes, while the length–weight conversion coefficient (LWYBB) had a negative effect. This effect was much more pronounced for the length and weight variables compared to the growth variable. On DOY 160, turbulent velocity (WA), pause duration–larval length function coefficient under conditions of no turbulence and low prey density (PD1A), and reactive distance–length relationship slope coefficient (RDA) had positive effects on growth, length, and weight, with RDA having the largest effect. Probability of prey capture for 15–16 mm larvae (PNAUP11), length–weight conversion coefficient (LWYBB), and routine metabolism power coefficient (MROFDLB) had negative effects on growth, length and weight. The values of the correlation coefficients were smaller compared to DOY 130, and there was also a wider range of important input parameters.

Within the mortality process, base mortality (MFDLSM) on DOY 130 had a positive effect on the total mortality variable ($r = 0.57$) and a corresponding negative effect on numbers ($r = -0.73$). Similarly, the mortality–length function slope coefficient (MSIZEB1) had a positive effect on numbers and a negative effect on total mortality. The length–weight conversion parameter (LWYBB) had a positive effect on predation mortality and an equal negative effect on starvation mortality. This result was caused by predation mortality being calculated by the difference between total and starvation mortality. On DOY 160 the values of the correlation coefficients were smaller compared to DOY 130. Input parameters having a positive effect on mortality processes were similar to DOY 130, except that feeding depth (FDEPTHG) was important to starvation mortality. Parameters having a negative effect on mortality processes included two prey capture probability parameters for 11–14 mm larvae (PNAUP7 and PEGGS9). Of the parameters having a negative effect on mortality processes, base mortality for small larvae (MFDLSM) on numbers had the greatest effect.

Within the consumption process, there was a surprising uniformity in the effect (magnitude and direction of the correlation coefficient) of input parameters on the cumulative feeding and the probability of successful pursuit output variables. The trends held up over both days and for both small and large larval comparisons. Reactive distance–length relationship slope (RDA), minimum pursuit time (t), and feeding depth (FDEPTHG) were the three most important input parameters. RDA had a uniform positive effect of similar magnitude and minimum pursuit time and feeding depth had negative effects of similar magnitude.

Discussion

Sundby and Fossum (1990) speculate that there should be an optimal level of turbulence with respect to the number of successful attacks larvae can inflict on their prey. Above such a level, successful attacks should

Table 3. Sensitivity of output variables to input parameters organized by process, day of the year, and magnitude and direction of the effect.

| | Input parameter | | | | | |
| | DOY 130 | | | DOY 160 | | |
Output variable	Positive r		Negative r	Positive r		Negative r
Growth						
MGR	RDA	0.33	LWYBB -0.25	WA	0.16	PNAUP11 -0.18
MLEN	RDA	0.32	LWYBB -0.59	PD1A	0.18	LWYBB -0.32
MWT	RDA	0.32	LWYBB -0.59	RDA	0.24	MROFDLB -0.28
Mortality						
MZ	MFDLSM	0.57	MSIZEB1 -0.32	MFDLSM	0.46	PNAUP7 -0.16
MPZ	LWYBB	0.42	MSIZEB1 -0.26	LWYBB	0.39	PEGGS9 -0.19
MSZ	MFDLSM	0.25	LWYBB -0.42	FDEPTHG	0.35	PEGGS9 -0.19
NUMBER	MSIZEB1	0.24	MFDLSM -0.73	MSIZEB1	0.31	MFDLSM -0.36
Consumption						
MCFSL	RDA	0.42	FDEPTHG -0.30	RDA	0.24	FDEPTHG -0.25
MCFLL	RDA	0.33	LWYBB -0.27	RDA	0.23	FDEPTHG -0.19
MPSSL	RDA	0.54	MPT -0.48	RDA	0.28	MPT -0.34
PMSLL	RDA	0.52	MPT -0.46	RDA	0.26	MPT -0.32

decrease because the residence time of the prey within the range of attack will be shorter than the reaction time of the predator, causing the prey to pass the predator before it is able to react. They speculate that this optimum should occur at windspeeds higher than 6 m s^{-1}. Results from our simulation (Figure 4) indicate that optimum feeding takes place at 7.2 m s^{-1}, which seems close and supports the theory.

Sundby (1995, 1997) argued that the negative effects of turbulence on larval feeding might not be an issue because windspeeds necessary to cause feeding to fall to the right of the consumption–turbulence optimum are rare. His statement is based on the model results reported in MacKenzie et al. (1994) that optimum feeding occurs at windspeeds of about 15 m s^{-1} and his observation (Sundby, 1995) that windspeeds off the coast of Norway do not typically reach that level. Our results, which are specific to 1987, also indicate that windspeeds in excess of 15 m s^{-1} are rare in Shelikof Strait. However, Brower et al. (1988) show that windspeeds in Shelikof Strait often exceed 15 m s^{-1}, doing so 13% of the time in April and 6% of the time in May.

Sundby (1995) recognized minimum pursuit time (t) as a critical parameter in the turbulence–consumption model of MacKenzie et al. (1994), who used a range of values (t=0.9, 1.7, and 2.6 s). The value of t used in our model was a random variable from a triangular distribution within a similar range (mean: 1.7; minimum: 0.85 s; maximum: 2.55 s). Sundby (1995) concluded that the windspeed generating a turbulence that optimizes ingestion depends on the assumed value of t and reported values of 10 m s^{-1} for t=2.6 s, 15.3 m s^{-1} for t=1.7 s, and 20 m s^{-1} for t=0.9 s. We expected optimum consumption rates from our model at windspeeds

somewhere in the range $10–20 \text{ m s}^{-1}$, mainly because we used a mean pursuit time of 1.7 s^{-1} in our simulations and our model basically replicated the physics and parameters of MacKenzie et al. (1994). However, our results indicate that optimum feeding occurs at a windspeed of 7.2 m s^{-1}. We believe this may be due to two factors. First, our formulation of the turbulence–consumption process is stochastic. Many of the deterministic values used by MacKenzie et al. (1994), such as minimum pursuit time, turbulent dissipation and turbulent velocity equation coefficients, pause frequency, and reactive distance–length parameters were random variables in our simulations. Secondly, our formulation of the feeding process is more complex, because we consider a pause-travel larval predator instead of a cruise predator as well as include a size-dependent prey capture probability for 14 prey groups covering three major life stages, each with different nutritional characteristics, and prey density values based on modelled observations. It appears that this additional complexity has the tendency to reduce the windspeed at which optimum feeding would take place. If our approach is valid, then negative affects of windspeed on larval feeding might be common.

Of the input parameters that influenced many output variables, two were associated with the turbulence/feeding formulations (RDA and WA), two with consumption processes (FDEPTHG and MAXPREYA), two with growth and bioenergetics processes (LWYBB and MROFDLB), and one with mortality (MFDLSM). Metamorphosis date, starvation, and predation mortality were the most sensitive to input parameters because these variables integrate a host of biophysical processes. The importance of feeding depth is caused by the decreasing prey concentration with depth and the

generally accepted decrease in wind-induced turbulence through the mixing layer (Yamazaki and Kamykowski, 1991). MacKenzie and Leggett (1993) also show that the influence of turbulence on the encounter rate between larvae and their prey decreases with depth in the mixed layer because of the decreasing rate of turbulent dissipation energy. Our results suggest that the importance of feeding depth results from the complex interplay between depth-dependent prey concentration and the change in the rate of turbulent energy dissipation with depth.

Two parameters of the encounter rate model, minimum pursuit time and reactive distance, played an important role in affecting feeding, growth, and mortality processes. This is confirmed by the observation by Werner *et al.* (1995) that a decrease in the time required for a larvae to pursue and capture a prey particle as it is being advected through the larvae's visual field increases growth and survival. Also, the weight–length parameters were important input variables affecting the turbulence–consumption process. Letcher *et al.* (1996) also reported the importance of larval length–weight conversion parameters, especially in highly size-dependent formulations, such as those described here. Fortunately, data on larval length–weight relationship parameters are relatively easy and inexpensive to obtain.

Our model clearly leaves many unanswered questions. Are other components of the predation process affected by turbulence? What are the relative effects of turbulence on prey encounter and probability of successful pursuit, its effects on timing of the prey-production cycle, on dilution or maintenance of prey patches, or on wind-induced changes in the mixed layer? Does turbulence compromise the prey's ability to perceive the presence of the predator? Are there turbulence-induced behavioural changes (swimming speed, turn angles, or avoidance) in larvae and prey? For example, Munk and Kiørboe (1985) have shown that herring larvae are capable of altering their swimming behaviour after encountering a prey patch so as to improve the likelihood of remaining in the patch. Results could change drastically if these factors had been included in the simulation model. Also unresolved is the issue of whether we selected the appropriate output variables.

Even with the above questions unanswered, this study demonstrates clearly that simulation modelling is a viable way to explore the complex issues related to turbulence, its effect on the biophysical environment and ultimately on growth and recruitment of fish larvae. Modelling provides a framework with which to examine the complex relationships concerned with the effect of turbulence on the ability of larval fishes to encounter, detect, pursue, and capture prey as well as a tool to move forward our understanding of the important biophysical couplings that occur at the scales relevant to larval fish and their prey.

Results of this study argue for more research on interactions between fish larvae and their prey, especially individual processes at very fine scales (such as larval reactive distance) and the conditions of the *in situ* feeding environment in turbulent conditions. In addition, features such as a larva's ability to pursue and encounter prey should be an important component of larval growth and survival models.

Acknowledgements

References

Bailey, K. M., Picquelle, S. J., and Spring, S. M. 1996. Mortality of larval walleye pollock *Theragra chalcogramma* in the western Gulf of Alaska, 1988–1991. Fisheries Oceanography, 5(Suppl 1): 124–136.

Brower, W. A., Baldwin, C. N., Wise, R. L., and Leslie, J. D. 1988. Climatic Atlas of the Outer Continental Shelf Waters and Coastal Regions of Alaska, vol. 1. NOAA, Arctic Environmental Information Data Center, Gulf of Alaska. 519 pp.

Canino, M. F., and Bailey, K. M. 1995. Gut evacuation of walleye pollock larvae in response to feeding conditions. Journal of Fisheries Biology, 46: 389–403.

Cury, P., and Roy, C. 1989. Optimal environmental window and pelagic fish recruitment success in upwelling areas. Canadian Journal of Fisheries and Aquatic Sciences, 46: 670–680.

Cury, P., Roy, C., Mendelssohn, R., Bakun, A., Husby, D. M., and Parrish, R. H. 1995. Moderate is better: exploring nonlinear climatic effects on the Californian northern anchovy (*Engraulis mordax*). *In* Climate Change and Northern Fish Populations, pp. 417–424. Ed. by R. J. Beamish. Canadian Special Publications in Fisheries and Aquatic Sciences, 121.

DeAngelis, D. L., and Gross, L. J. 1992. Individual-based models and approaches in ecology: populations, communities, and ecosystems. Routledge, Chapman and Hall Inc, New York. 525 pp.

Dower, J. F., Miller, T. J., and Leggett, W. G. 1997. The role of microscale turbulence in the feeding ecology of larval fishes. Advances in Marine Biology, 31: 169–220.

Frost, B. W. 1987. Grazing control of phytoplankton stock in the open subarctic Pacific Ocean: a model assessing the role of mesozooplankton, particularly the large calanoid copepods *Neocalanus* spp. Marine Ecology Progress Series, 39: 49–68.

Frost, B. W. 1993. A modelling study of processes regulating plankton standing stock and production in the open subarctic Pacific Ocean. Progress in Oceanography, 32: 17–56.

Gardner, R. H., Rojder, B., and Bergstrom, U. 1983. PRISM: A systematic method for determining the effect of parameter uncertainties on model predictions. Tech. NW-83/555, Studvik, Energetik. AB, Nyköping, Sweden.

Gargett, A. E. 1989. Ocean turbulence. Annual Review of Fluid Mechanics, 21: 419–451.

Hermann, A. J., and Stabeno, P. J. 1996. An eddy resolving model of the circulation of the western Gulf of Alaska shelf. Journal of Geophysical Research, 101: 1129–1149.

Hinckley, S. 1999. Biophysical mechanisms underlying the recruitment process in walleye pollock (*Theragra chalcogramma*). PhD dissertation, University of Washington, Seattle. 258 pp.

Hinckley, S., Hermann, A. J., and Megrey, B. A. 1996. Development of a spatially explicit, individual-based model of marine fish early life history. Marine Ecology Progress Series, 139: 47–68.

Hinckley, S., Herman, A. J., Mier, K., and Megrey, B. A. 2001. The importance of spawning location and timing to successful transport to nursery areas: a simulation modelling study of Gulf of Alaska walleye pollock. ICES Journal of Marine Science, 58: 1043–1053 (This volume).

Huston, M. A., DeAngelis, D. L., and Post, W. M. 1988. New computer models unify ecological theory. BioScience, 38: 682–691.

Judson, O. P. 1994. The rise of the individual-based model in ecology. Trends in Ecology and Evolution, 9: 9–14.

Kendall, A. W., Clarke, M. E., Yoklovich, M. M., and Bohlert, G. W. 1987. Distribution, feeding, and growth of larval walleye pollock, *Theragra chalcogramma*, from Shelikof Strait, Gulf of Alaska. Fisheries Bulletin, US, 85: 499–521.

Lackman, G. M., and Overland, J. E. 1989. Atmospheric structure and momentum balance during a gap-wind event in Shelikof Strait, Alaska. Monthly Weather Review, 116: 1817–1833.

Lasker, R. 1975. Field criteria for survival of anchovy larvae: the relation between inshore chlorophyll maximum layers and successful first feeding. Fisheries Bulletin, US, 73: 453–462.

Letcher, B. H., Rice, J. A., Crowder, L. B., and Rose, K. A. 1996. Variability in survival of larval fish: disentangling components with a generalized individual-based model. Canadian Journal of Fisheries and Aquatic Sciences, 53: 787–801.

MacKenzie, B. R., and Leggett, W. C. 1993. Wind-based models for estimating the dissipation rates of turbulent energy in aquatic environments: empirical comparisons. Marine Ecology Progress Series, 94: 207–216.

MacKenzie, B. R., and Kiørboe, T. 1995. Encounter rates and swimming behaviour of pause-travel and cruise larval fish predators in calm and turbulent laboratory environments. Limnology and Oceanography, 40: 1278–1289.

MacKenzie, B. R., Miller, T. J., Cyr, S., and Leggett, W. C. 1994. Evidence for a dome-shaped relationship between turbulence and larval fish ingestion rates. Limnology and Oceanography, 39: 1790–1799.

Macklin, S. A., Stabeno, P. J., and Schumacher, J. D. 1993. A comparison of gradient and observed over-the-water winds along a mountainous coast. Journal of Geophysical Research, 98: 16555–16569.

Marasse, C., Costello, J. S., Granata, T., and Strickler, J. R. 1990. Grazing in a turbulent environment: energy dissipation, encounter rates and the efficacy of feeding currents in *Centropages hamatus*. Proceedings of the National Academy of Science, 87: 1653–1657.

Matsushita, K. 1991. How do fish larvae of limited motility encounter nauplii in the sea. *In* Proceedings of the 4th International Conference on Copepoda, pp. 251–270. Bulletin of Plankton Society of Japan, Special Volume.

McKay, M. D., Beckman, R. D., and Conover, W. J. 1979. A comparison of three methods for selecting values of input variables in the analysis of output from computer code. Technometrics, 21: 239–245.

Munk, P., and Kiørboe, T. 1985. Feeding behaviour and swimming activity of larval herring (*Clupea harengus*) in relation to density of copepod nauplii. Marine Ecology Progress Series, 24: 15–21.

Nishiyama, T., Hirano, K., and Haryu, T. 1983. The early life history and feeding habit of larval walleye pollock, *Theragra chalcogramma* (Pallas) in the Southeast Bering Sea. INPFC Groundfish Symposium Paper No. P-10.

Paul, A. J. 1983. Light, temperature, nauplii concentrations, and prey capture by first feeding pollock larvae *Theragra chalcogramma*. Marine Ecolology Progress Series, 13: 175–179.

Perterman, R. M., and Bradford, M. J. 1987. Wind speed and mortality of a marine fish, the Northern anchovy (*Engraulis mordax*). Science, 235: 354–356.

Rose, K. A. 1981. Sensitivity analysis in ecological simulation models. *In* Systems and Control Encyclopedia, Theory, Technology, Applications. pp. 4230–4235. Ed. by M. G. Singh.

Rose, K. A., Smith, E. P., Gardner, R. H., Brenkert, A. L., and Bartell, S. M. 1991. Parameter sensitivities, Monte Carlo filtering, and model forecasting under uncertainty. Journal of Forecasting, 10: 117–133.

Rose, K. A., Christensen, S. W., and DeAngelis, D. L. 1993. Individual-based modeling of populations with high mortality: a new method based on following a fixed number of model individuals. Ecological Modeling, 68: 273–292.

Rothschild, B. R., and Osborn, T. R. 1988. Small-scale turbulence and plankton contact rates. Journal of Plankton Research, 10: 465–474.

Scheffer, M., Baveco, J. M., DeAngelis, D. L., Rose, K. A., and Van Nes, E. H. 1995. Super-individuals: a simple solution for modelling large populations on an individual basis. Ecological Modeling, 80: 161–170.

Stabeno, P. J., Hermann, A. J., Bond, N. A., and Bograd, S. J. 1995. Modeling the impact of climate change variability on the advection of larval walleye pollock (*Theragra chalcogramma*) in the Gulf of Alaska. *In* Climate Change and Northern Fish Populations, pp. 719–727. Ed. by R. J. Beamish. Canadian Special Publication on Fisheries and Aquatic Sciences, 121.

Sundby, S. 1995. On the dome-shaped relationship between wind-generated turbulence and larval feeding. Netherlands Journal of Sea Research, 34: 243–244.

Sundby, S. 1997. Turbulence and ichthyoplankton: influence on vertical distributions and encounter rates. Scientia Marina, 61(Suppl 1): 159–176.

Sundby, S., and Fossum, P. 1990. Feeding conditions of Arcto-Norwegian cod larvae compared with the Rothschild–Osborn theory on small-scale turbulence and plankton contact rates. Journal of Plankton Research, 12: 1153–1162.

Sundby, S., Ellertsen, B., and Fossum, P. 1994. Encounter rates between first feeding cod larvae and their prey during moderate to strong turbulent mixing. ICES Marine Science Symposia, 198: 393–405.

Tilseth, S. 1984. The distribution of cod larvae and prey organisms in the Lofoten area related to critical prey concentrations. *In* Proceedings of the Soviet–Norwegian symposium on reproduction and recruitment of Arctic Cod, pp. 36–71. Ed. by O. R. Godo, and S. Tilseth. Institute of Marine Research, Bergen, Norway.

Torres, J. J., and Childress, J. J. 1983. Relationship of oxygen consumption to swimming speed in *Euphausia pacifica*. 1.

Effects of temperature and pressure. Marine Biology, 74: 79–86.

Werner, F. E., Perry, R. I., MacKenzie, B. R., Lough, R. G., and Naimie, C. E. 1995. Larval trophodynamics, turbulence, and drift on Georges Bank: a sensitivity analysis of cod and haddock. ICES CM 1995/Q: 26.

Yamazaki, H., and Kamykowski, D. 1991. The vertical trajectories of motile phytoplankton in a wind-mixed water column. Deep-Sea Research, 38: 219–241.

Appendix

Appendix 1. Input parameters for the individual-based model (IBM) and nominal values used to generate random variates from a triangular probability distribution (Ps: *Pseudocalanus* ssp.; cop: copepodite stage; nau: naupliar stage; l: length; ll: larval length; w: weight; dw: dry weight; pd: prey density; c: coefficient; par: parameter; prob: probability).

Input par	Description	Mean	Minimum	Maximum
AELARV	Larval assimilation efficiency	0.8	0.6	0.9
BIGPD	Pause duration (s) for larvae >25 days old	0.1	0.05	0.15
CALM	Turbulent velocity defining calm vs. turbulent conditions ($m^2 s^{-3}$)	7.40×10^{-8}	3.70×10^{-8}	1.11×10^{-7}
COPSPEED	Swimming speed of Ps cop ($m s^{-1}$)	0.0004503	0.0002252	0.0006755
CRITKFDL	Critical condition factor defining onset of starvation	0.4	0.25	0.5
DWTC1	dw of 1st Ps cop (mg)	7.20×10^{-4}	0.00036	0.00108
DWTC2	dw of 2nd Ps cop (mg)	1.20×10^{-3}	0.0006	0.0018
DWTC3	dw of 3rd Ps cop (mg)	2.00×10^{-3}	0.001	0.003
DWTC4	dw of 4th Ps cop (mg)	3.40×10^{-3}	0.0017	0.0051
DWTC5	dw of 5th Ps cop (mg)	6.00×10^{-3}	0.003	0.009
DWTC6	dw of 6th Ps cop (mg)	8.00×10^{-3}	0.004	0.012
DWTEGG	dw of Ps egg (mg)	7.00×10^{-5}	0.000035	0.000105
DWTN1	dw of 1st Ps nau (mg)	8.00×10^{-5}	0.00004	0.00012
DWTN2	dw of 2nd Ps nau (mg)	8.00×10^{-5}	0.00004	0.00012
DWTN3	dw of 3rd Ps naue (mg)	1.80×10^{-4}	0.00009	0.00027
DWTN4	dw of 4th Ps nau (mg)	2.70×10^{-4}	0.000135	0.000405
DWTN5	dw of 5th Ps nau (mg)	4.00×10^{-4}	0.0002	0.0006
DWTN6	dw of 6th Ps nau (mg)	6.40×10^{-4}	0.00032	0.00096
ENDFEED	Hour of day when feeding ends (h)	22	11	33
ETAA	Intercept turbulence dissipation rate function[1]	5.82×10^{-9}	2.91×10^{-9}	8.73×10^{-9}
FDEPTHG	Depth of feeding larvae (m)	25	15	50
FDLACTMULT	Activity multiplier[2]	2	1.5	3
HRLIGHT	Hours of daylight (h)	16	6	18
LOWPREY	Low prey density definition (no. m^{-3})	35 000	5000	40 000
LWBSA	L-w conversion par[2]	0.3266	0.1633	0.4899
LWBSB	L-w conversion par[2]	3.395	1.6975	5.0925
LWYBA	L-w conversion par[4]	0.1754	0.0877	0.2631
LWYBB	L-w conversion par[4]	3.615	1.8075	5.4225
MAXPREYA	Intercept ll-maximum prey size function	0.115	0.0575	0.1725
MAXPREYB	Slope ll-maximum prey size function	0.235	0.1175	0.3525
MFDLSM	Base mortality when ll <7.0 mm (d^{-1})	0.1	0.05	0.2
MFNFDLA	Intercept feeding metabolism-w function[4]	0.00308	0.00154	0.00462
MFNFDLB	Power c feeding metabolism-w function	0.9059	0.45295	1.35885
MINMORT	Minimum mortality (d^{-1})	0.02	0.001	0.05
MROFDLB	Power c routine metabolism-w function[4]	0.9699	0.48495	1.45485
MSIZEA1	Proportional c mortality-l function, 1987	1.7007	0.85035	2.55105
MSIZEB1	Slope mortality-l function for 1987	2.0312	1.0156	3.0468
MSIZEB6	Slope mortality-l function for average year	4.9738	2.4869	7.4607
NAUPSPEED	Swimming speed Ps nau ($m s^{-1}$)	0.0001054	0.0000527	0.0001581
OLDMORT	Mortality when age >25 days old (d^{-1})	0.02	0.001	0.05
PCOP1	Prob. of larvae <6 mm eating a Ps cop	0.015	0.00075	0.01575
PCOP2	Prob. of 6–7 mm larvae eating a Ps cop	0.02	0.001	0.021
PCOP3	Prob. of 7–8 mm larvae eating a Ps cop	0.015	0.00075	0.01575
PCOP4	Prob. of 8–9 mm larvae eating a Ps cop	0.008	0.0004	0.0084
PCOP5	Prob. of 9–10 mm larvae eating a Ps cop	0.025	0.00125	0.02625
PCOP6	Prob. of 10–11 mm larvae eating a Ps cop	0.048	0.0024	0.0504
PCOP7	Prob. of 11–12 mm larvae eating a Ps cop	0.099	0.00495	0.10395
PCOP8	Prob. of 12–13 mm larvae eating a Ps cop	0.192	0.1824	0.2016
PCOP9	Prob. of 13–14 mm larvae eating a Ps cop	0.236	0.2242	0.2478
PCOP10	Prob. of 14–15 mm larvae eating a Ps cop	0.217	0.20615	0.22785
PCOP11	Prob. of 15–16 mm larvae eating a Ps cop	0.337	0.32015	0.35385

Appendix 1. Continued

Input par	Description	Mean	Minimum	Maximum
PCOP12	Prob. of 16–17 mm larvae eating a Ps cop	0.348	0.3306	0.3654
PCOP13	Prob. of 17–19 mm larvae eating a Ps cop	0.875	0.83125	0.91875
PCOP14	Prob. of larvae >19 mm eating a Ps cop	0.873	0.82935	0.91665
PD1A	Intercept pd-ll function calm/low pd	2.522	1.261	3.783
PD1B	Slope pd-ll function calm/low pd	0.111	0.0555	0.1665
PD2A	Intercept pd-ll function calm/high pd	24.267	12.1335	36.4005
PD2B	Slope pd-ll function calm/high pd	3.667	1.8335	5.5005
PD3A	Intercept pd-ll function turbulent/low pd	5.189	2.5945	7.7835
PD3B	Slope pd-ll function turbulent/low pd	0.556	0.278	0.834
PD4A	Intercept pd-ll function turbulent/high pd	10.111	5.0555	15.1665
PD4B	Slope pd-ll function turbulent/high pd	1.444	0.722	2.166
PEGGS1	Prob. of a pollock larvae <6 mm eating a Ps egg	0.015	0.00075	0.01575
PEGGS2	Prob. of 6–7 mm larvae eating a Ps egg	0.02	0.001	0.021
PEGGS3	Prob. of 7–8 mm larvae eating a Ps egg	0.015	0.00075	0.01575
PEGGS4	Prob. of 8–9 mm larvae eating a Ps egg	0.03	0.0015	0.0315
PEGGS5	Prob. of 9–10 mm larvae eating a Ps egg	0.015	0.00075	0.01575
PEGGS6	Prob. of 10–11 mm larvae eating a Ps egg	0.053	0.00265	0.05565
PEGGS7	Prob. of 11–12 mm larvae eating a Ps egg	0.156	0.1482	0.1638
PEGGS8	Prob. of 12–13 mm larvae eating a Ps egg	0.327	0.31065	0.34335
PEGGS9	Prob. of 13–14 mm larvae eating a Ps egg	0.35	0.3325	0.3675
PEGGS10	Prob. of 14–15 mm larvae eating a Ps egg	0.624	0.5928	0.6552
PEGGS11	Prob. of 15–17 mm larvae eating a Ps egg	0.382	0.3629	0.4011
PEGGS12	Prob. of 16–17 mm larvae eating a Ps egg	0.01	0.0005	0.0105
PEGGS13	Prob. of 17–19 mm larvae eating a Ps egg	0.01	0.0005	0.0105
PEGGS14	Prob. of larvae >19 mm eating a Ps egg	0.01	0.0005	0.0105
PF	Pause frequency (s^{-1})	0.52	0.2	0.75
PNAUP1	Prob. of a larvae <6 mm eating a Ps nau	0.97	0.9025	0.9975
PNAUP2	Prob. of 6–7 mm larvae eating a Ps nau	0.96	0.9025	0.9975
PNAUP3	Prob. of 7–8 mm larvae eating a Ps nau	0.97	0.9025	0.9975
PNAUP4	Prob. of 8–9 mm larvae eating a Ps nau	0.96	0.9025	0.9975
PNAUP5	Prob. of 9–10 mm larvae eating a Ps nau	0.95	0.9025	0.9975
PNAUP6	Prob. of 10–11 mm larvae eating a Ps nau	0.899	0.85405	0.94395
PNAUP7	Prob. of 11–12 mm larvae eating a Ps nau	0.745	0.70775	0.78225
PNAUP8	Prob. of 12–13 mm larvae eating a Ps nau	0.481	0.45695	0.50505
PNAUP9	Prob. of 13–14 mm larvae eating a Ps nau	0.414	0.3933	0.4347
PNAUP10	Prob. of a 14–15 mm larvae eating a Ps nau	0.159	0.15105	0.16695
PNAUP11	Prob. of a 15–16 mm larvae eating a Ps nau	0.281	0.26695	0.29505
PNAUP12	Prob. of a 16–17 mm larvae eating a Ps nau	0.642	0.6194	0.6846
PNAUP13	Prob. of 17–19 mm larvae eating a Ps nau	0.115	0.11875	0.13125
PNAUP14	Prob. of larvae >19 mm eating a Ps nau	0.117	0.12065	0.13335
PREYLENC1	Median carapace l of 1st Ps cop (mm)	0.528725	0.2643625	0.7930875
PREYLENC2	Median carapace l of 2nd Ps cop (mm)	0.701531	0.3507655	1.0522965
PREYLENC3	Median carapace l of 3rd Ps cop (mm)	0.779336	0.389668	1.169004
PREYLENC4	Median carapace l of 4th Ps cop (mm)	1.02197	0.510985	1.532955
PREYLENC5	Median carapace l of 5th Ps cop (mm)	1.27041	0.635205	1.905615
PREYLENC6	Median carapace l of 6th Ps cop (mm)	1.53912	0.76956	2.30868
PREYLENEGG	Median Ps egg diameter (mm)	0.13	0.065	0.195
PREYLENN1	Median carapace l of 1st Ps nau (mm)	0.1419	0.07095	0.21285
PREYLENN2	Median carapace l of 2nd Ps nau (mm)	0.1506	0.0753	0.2259
PREYLENN3	Median carapace l of 2nd Ps nau (mm)	0.1868	0.0934	0.2802
PREYLENN4	Median carapace l of 2nd Ps nau (mm)	0.2347	0.11735	0.35205
PREYLENN5	Median carapace l of 2nd Ps nau (mm)	0.2728	0.1364	0.4092
PREYLENN6	Median carapace l of 2nd Ps nau (mm)	0.2888	0.1444	0.4332
Q10L	Q10 bioenergetic processes [Hinckley *et al.*, 1996: (7), (8), (9)]	2	1.75	3
RDA	Slope of reactive distance-l relationship (mm)	0.769	0.3845	1.1535
STARTFEED	Hour of day when feeding starts (h)	5	2.5	7.5
t	Minimum pursuit time (s)	1.7	0.85	2.55
WA	Proportional turbulent velocity c[5]	3.615	1.8075	5.4225

[1]See Equation 10 in MacKenzie *et al.*, 1994.
[2]See Equation 10 in Hinckley *et al.*, 1996.
[3]See Equation 13 in Hinckley *et al.*, 1996.
[4]See Equation 8 in Hinckley *et al.*, 1996.
[5]See Equation 4 in MacKenzie and Kiørboe, 1995.